International Journal of Pharmaceutics 545 (2018) 366–377

Contents lists available at ScienceDirect

International Journal of Pharmaceutics

journal homepage: www.elsevier.com/locate/ijpharm

Polysaccharides-based multiparticulated interpolyelectrolyte complexes for controlled benznidazole release

Mónica C. García[a,b], Rubén H. Manzo[a,b], Alvaro Jimenez-Kairuz[a,b,*]

[a] Departamento de Ciencias Farmacéuticas, Facultad de Ciencias Químicas, Universidad Nacional de Córdoba, Córdoba, Argentina
[b] Unidad de Investigación y Desarrollo en Tecnología Farmacéutica – UNITEFA (CONICET-UNC), Argentina

ARTICLE INFO

Keywords:
Benznidazole
Chitosan
Alginic acid
Polyelectrolyte complexes
Drug delivery

ABSTRACT

Polysaccharides-based delivery systems and interpolyelectrolyte complexes (IPECs) are interesting alternatives to control the release of drugs, thereby improving therapies. Benznidazole (BZ) is the selected drug for Chagas disease pharmacotherapy. However, its side effects limit its efficacy and safety. We developed novel multiparticulated BZ-loaded IPECs based on chitosan and alginic acid, and investigated their physicochemical and pharmacotechnical properties. IPECs were obtained using the casting solvent method, followed by wet granulation. They presented ionic interaction between the biopolymers, revealed that free BZ was uniformly distributed and showed adequate flow properties for hard gelatin-capsule formulation. The multiparticles exhibited mucoadhesion properties and revealed modulation of BZ release, depending on the release media, in accordance with the fluid uptake. The IPECs developed possess interesting properties that are promising for the design of novel alternatives to improve Chagas disease pharmacotherapy, which would diminish BZ's adverse effects and/or allow a reduction in the frequency of BZ administration.

1. Introduction

Chagas disease, caused by *Trypanosoma cruzi,* has become a serious global health problem that has spread to non-endemic countries (Cencig et al., 2012; Rassi et al., 2012; Rassi et al., 2010). To date, the efficacy and safety of Chagas disease pharmacotherapy is still unsatisfactory (García et al., 2016), and is mainly based on two drugs developed five decades ago, benznidazole (BZ; Radanil®, La Roche and Abarax®, Elea, Arg.) and nifurtimox (NFX; Lampit®, Bayer) (Bellera et al., 2015). Pharmacotherapy with these drugs is characterized by poor compliance, especially in adult patients, due to the high dose and long-term treatment, frequent undesirable side effects, and biochemical damage to mammalian tissues (Davies et al., 2014). However, it has been proposed that BZ is better tolerated than NFX (Rassi et al., 2010; Rojo et al., 2014).

The field of pharmaceutical technology designs novel strategies that contribute to the development of new controlled drug release systems and/or new formulations for existing approved drugs (Bermudez et al., 2016; Chatelain and Ioset, 2011). They can be used to improve many negative aspects of the current pharmacological treatment of Chagas disease. The rationale for developing delivery systems includes extending the duration of action of the drug, reducing the frequency of dosing, and improving therapeutic efficacy by providing a constant drug level, thereby overcoming adverse side effects (Pagels and Prud'homme, 2015). Even when several BZ delivery systems have been described, many of which are based on the use of polysaccharides, including cyclodextrins complexes (de Melo et al., 2016; Leonardi et al., 2013; Soares-Sobrinho et al., 2012), microparticles of chitosan (Leonardi et al., 2009), solid dispersions of low-substituted hydroxypropyl cellulose (Fonseca-Berzal et al., 2015; Palmeiro-Roldán et al., 2014), oil/water emulsions (Streck et al., 2014), liposomal formulations (Morilla et al., 2002; Morilla et al., 2004), and BZ microcrystals (Leonardi et al., 2009; Maximiano et al., 2011); the use of interpolyelectrolyte complexes (IPECs) has been poorly explored.

Polyelectrolytes (PE) are charged polyelectrolytes that can interact electrostatically in aqueous media to form soluble or insoluble IPECs. This approach has received much attention in recent years (Bani-Jaber et al., 2011; Moustafine et al., 2011; Obeidat et al., 2008; Prado et al., 2008). IPECs are capable of more sustained drug release than single biopolymers (Bani-Jaberm et al., 2011; Jeganathan and Prakya, 2015), and they have been used in a large variety of pharmaceutical applications (AlHusban et al., 2011; Auriemma et al., 2013; Dey et al., 2008; Pan et al., 2010; Severino et al., 2012). Among the research on the use of IPECs for controlled drug release, the following systems have been emphasized: Eudragit® E100-sodium alginate (Moustafine et al., 2005), Chitosan (CH)-Eudragit® L100 (Moustafine et al., 2008), and Eudragit®

* Corresponding author at: Haya de la Torre y Medina Allende, Edificio Ciencias 2, Ciudad Universitaria (5000), Córdoba, Argentina.
E-mail addresses: mgarcia@fcq.unc.edu.ar (M.C. García), rubmanzo@fcq.unc.edu.ar (R.H. Manzo), alvaro@fcq.unc.edu.ar (A. Jimenez-Kairuz).

https://doi.org/10.1016/j.ijpharm.2018.05.017
Received 8 February 2018; Received in revised form 24 April 2018; Accepted 6 May 2018
Available online 07 May 2018
0378-5173/

EPO-Kappa carrageenan (Prado et al., 2008), and they are demonstrated interesting properties for use as drug delivery systems, which can be explored for controlled BZ delivery.

In particular, CH is a natural polysaccharide derivative of chitin that has been studied for several purposes in the biomedical field (Thakur and Thakur, 2014; Zargar et al., 2015). CH-based materials have received attention because of their unique properties, namely biodegradability, biocompatibility, non-toxicity, and antibacterial activity (Ahmed and Aljaeid, 2016; Kong et al., 2010; Raafat and Sahl, 2009). Alginic acid (AA) is another polyelectrolyte with potential; it is a naturally occurring hydrophilic colloidal polysaccharide consisting mainly of residues of D-mannuronic acid and L-glucuronic acid, obtained from various species of brown seaweed (Karbassi et al., 2014). This biopolymer is an effective polyanion and is readily associable with many molecules through ionic interactions or covalent bonds (Ramirez-Rigo et al., 2006). The combination of CH and alginate has been reported for several purposes (Algul et al., 2015; Jabeen et al., 2016; Kim et al., 2015; Lacerda et al., 2014; Nista et al., 2015; Wang et al., 2014); however, information on the ionic interaction between CH and AA is still very limited, and there are no reports related to the use of these as carriers of BZ.

Considering the advantageous properties that IPECs exhibit, we hypothesize that these kinds of systems formulated as multiparticles would be promising carriers of BZ, which could improve the treatment of Chagas disease. As it is well known that multipaticulated systems offer numerous advantages over single-unit dosage forms, such as reduced risk of systemic toxicity, low risk of dose dumping, more uniform and reliable gastrointestinal transit, due to their multiplicity and small sizes, in which each particle can be considered a true drug delivery system (AlHusban et al., 2011; Auriemma et al., 2013; Dey et al., 2008; Pan et al., 2010; Severino et al., 2012). Moreover, controlled BZ release would reduce its adverse effects by avoiding high plasmatic BZ concentration and would allow a reduction in its frequency of administration. In addition, BZ is poorly soluble in water (García et al., 2015) which may have a direct impact on its oral bioavailability (Sá-Barreto et al., 2013). Thus, the development of novel biocompatible materials capable of overcoming the undesirable properties of BZ would therefore be useful in the preparation of oral solid formulations, with simple and low-cost manufacturing processes. These could provide an interesting approach for the development of new effective and safe forms of BZ dosage.

In this context, the goal of this work was to develop novel multiparticulated IPECs, based on polysaccharides (CH and AA), as carriers of BZ, and to investigate their pharmacotechnical properties for oral administration. Moreover, the physicochemical characterizations to evaluate the polymer-polymer and polymer-drug interactions were studied.

2. Materials and methods

2.1. Materials: drug, biopolymers and reagents

The benznidazole (BZ) was extracted and purified from commercially available tablets (Radanil®, Roche, Argentine), as reported in a previous work (García et al., 2016). Briefly, 100 tablets were crushed; the powder was transferred into a glass container and dispersed with 2 mL of ethanol per tablet under controlled heating (40–45 °C) and constant stirring for 30 min. Then, the dispersion was filtered and the remaining solid was discarded. BZ was recrystallized by the addition of 200 mL of cold distilled water under an ice bath condition. The solid was dried in an oven at 45 °C until constant weight and it was stored at room temperature in well-closed light resistant glass containers. The solid BZ was obtained with yield of 87 ± 2%. The analysis by Fourier transform infrared spectroscopy (FT-IR) showed the characteristics absorption bands of BZ and the differential scanning calorimetry (DSC) curves demonstrated narrow melting temperature range at 190.2–191.2 °C (Figs. 3 and 4, respectively). The quantification of BZ assayed by high-performance liquid chromatography with UV–visible detection exhibited 99.2 ± 0.5%p/p of BZ in the solid obtained, ensuring its quality as an active pharmaceutical ingredient. These results agree with an acceptable purity of BZ according to Pharmacopoeia specifications (World Health Organization, 2015).

Two polysaccharides: alginic acid (AA) from *Macrocystis pyrifera* (PA grade, Sigma Aldrich®) and chitosan (CH) (PA grade, Sigma Aldrich®) were used. The proportions of ionizable groups of these polyelectrolytes were determined by potentiometric titration and the equivalents of amino or carboxylic groups, expressed as mmol g^{-1} of polyelectrolytes (PE) were 5.11 and 4.40, respectively.

The following reagents: potassium phosphate monobasic (KH_2PO_4, PA grade, Anedra®),) and potassium phosphate dibasic (K_2HPO_4, PA grade, Anedra®), sodium chloride (NaCl, PA grade, Parafarm®), absolute ethanol (CH_3CH_2OH), 1 N sodium hydroxide (NaOH) and hydrogen chloride (HCl) solutions (Anedra®) were used as purchased without further purification.

Physiological solution (sodium chloride 0.9% w/v), simulated gastric solution without pepsin (SGS, to represent gastric pH in the fasted state), and phosphate buffer pH 6.8 (to represent intestinal pH), were prepared according to United States Pharmacopoeia (USP) specifications, using analytical grade reagents.

All experiments were carried out with distilled and purified water.

2.2. Preparation of polysaccharides-based interpolyelectrolyte complexes loaded with benznidazole

Two types of interpolyelectrolyte complexes (IPECs) were prepared, one of them obtained in water and the other in hydroalcoholic mixture as interaction media. The addition of AA was in stoichiometric proportions to neutralize all ionizable groups of CH. The BZ was incorporated in a ratio of 1:1 w/w respect to the total amount of IPEC.

To obtain the solid state of these systems the casting solvent method was employed. The solids of the two PE and BZ were put in contact in a mortar and the interaction medium was added in small aliquots. Water and hydroalcoholic mixture (1:1 H_2O: CH_3CH_2OH) were used as interaction media. With the addition of the interaction medium a semi-solid paste was formed, which was subjected to a mixing process during 10 min and left overnight at room temperature. The volume of media employed was 1.7 ± 0.2 and 1.5 ± 0.1 mL/g of solid, for water and hydroalcoholic medium, respectively. After 24 h, the material was dried at room temperature until the constant weight was achieved, monitored by mass determination on an analytical balance. It was considered constant when three successive determinations presented a mass variation less than 5%. The maximum time required to dry the IPECs was in average 72 h, which depends on the amount of solid to be processed. Once dry, the solid materials were milled and passed through 210 and 400 μm size pores of mesh sieves.

Finally, the systems based on BZ-loaded IPEC were obtained, both in water (subscript *w*) and in hydroalcoholic medium (subscript *h*), namely CH-AA-BZ_w y CH-AA-BZ_h.

Physical mixtures (PM) with composition equivalents to the IPEC were prepared by a simple mixing of the powders in a mortar of the two polysaccharides and BZ.

2.3. Solid processing to obtain multiparticulated benznidazole-loaded interpolyelectrolyte complexes

After sieving the solids obtained were processed to obtain the multiparticulated BZ-loaded IPECs. The wet granulation process was made as follow: each solid complex was placed in the mortar and it was moistened with 39 ± 2% of water respect to the total amount of solid. No additional binder agents were added. Only water was used as wetting agent. Then, the mass was manually extruded using a Teflon spatula through an 850–1000 μm metal mesh and the multiparticles

obtained were dried to constant weight in an oven at 40 °C.

The multiparticles were classified according to their particle size based on the analytical sieves used (mesh sieves: 1000–850 μm, 850–600 μm and ≤600 μm). The total amount of each fraction collected was summed and compared to the initial amount of solid used to obtain the IPEC, and the yield was determined. Also, the yield of each fraction collected was analyzed respect to the total amount of each multiparticulated system.

The different fractions collected (1000–850 μm, 850–600 μm and ≤600 μm) were packing in light-resistant glass containers for further characterization.

2.4. Yield

The multiparticles obtained were classified according to their particle size based on the sieves used. The total amount of each fraction collected as summed and compared to the initial amount of solid used to obtain the IPEC, and the yield was determined. Also, the yield of each fraction collected was analyzed respect to the total amount of each multiparticle.

Physicochemical and pharmacotechnical characterization were determined mainly from multiparticles with sizes in the range of 1000–850 μm, except to the comparison of release profiles of multiparticulated IPECs with different particle sizes.

2.5. Physicochemical characterization of benznidazole-loaded interpolyelectrolyte complexes

Solid products IPEC, CH, AA, BZ and its PM, were characterized through confocal microscopy, powder X-ray diffraction (PXRD), Fourier transform infrared spectroscopy (FT-IR) and thermal analysis.

Both IPECs were analyzed using a confocal reflection microscope (LEXT OLS4000 3D Confocal Laser Microscope, Olympus®, Latin America). Specific software (Lext OLS 4000 version 3.1.1v, Olympus Corp) was used to take and process the images. Samples were prepared by carefully placing the solid material on a slide. Images were obtained with an increase of 408X.

The PXRD patterns were acquired at room temperature on an X-ray diffractometer (PANalytical® X'Pert Pro, Holland) using Cu Ka radiation (λ = 1.5418 Å, tube operated at 40 kV, 100 mA). Data were collected over an angular range from 5 to 90° 2θ/θ in continuous scan mode, with a step size of 0.02° 2θ and a time counting of 5 s per step. The obtained diffractograms were analyzed by an X'Pert data viewer (PANanalytical, Holland).

FT-IR spectra were acquired on an infrared microscope (Nicolet iN10, Thermo Scientific®, USA). The samples were dried under vacuum for 2 h before the determination. Samples were scanned from 4000 to 400 cm^{-1} and the recording conditions were resolution, 8.0; sample scan, 40. The spectra were obtained, processed and analyzed using the program EZ OMNIC ESP 5.1.

Thermal behavior was evaluated by differential scanning calorimetry (DSC) and thermogravimetric analysis (TGA) in a TA®-instrument, Discovery series equipped with a data station (Trios® software, v4.1.1, TA Instruments). DSC was performed on samples (0.9–1.7 mg) heated in non-hermetic aluminum pans with a pine hole, using heating ramp of 10 °C/min from 15 to 200 °C, under N_2 flux (50 mL min^{-1}). TGA was performed on samples (approximately 2 mg) placed in open aluminum pans and heated from room temperature to 300 °C under the conditions used in DSC analysis.

2.6. Pharmacotechnical assays benznidazole-loaded multiparticulated interpolyelectrolyte complexes

2.6.1. Flow properties of particles

The flow properties of the multiparticulated IPECs were determined in order to select the solids with better flowability for further studies. The angle of repose (α) was determined according to Eq. (1).

$$tg(\alpha) = \frac{h}{r} \quad (1)$$

where h and r were height and base radius of the cone formed by the particles, respectively (Pérez et al., 2006). The bulk and tapped densities (δ_{bulk} and δ_{tap}, respectively) were measured in a 10-mL graduated cylinder. A known weight of particles (approximately 1 g) was introduced into the cylinder and the initial volume was recorded. Then, it was manually tapped (approximately 100 times) until a constant volume was reached, and the final volume was recorded. The δ_{bulk} was calculated as the ratio between the particles weight (g) and the initial volume (mL) and the δ_{tap} as the ratio between the particles weight (g) and the final volume (mL). From these results, the Carr's Index (CI %) and Hausner's ratio (H_R) were calculated according to Eqs. (2) and (3), respectively, which are parameters to determine the flow properties of solids (Vila Jato, 1997)

$$CI\ \% = \frac{\delta_{tap} - \delta_{bulk}}{\delta_{tap}} \times 100 \quad (2)$$

$$H_R = \frac{\delta_{tap}}{\delta_{bulk}} \quad (3)$$

All of these determinations were made using the methods described in the European Pharmacopoeia (Section 2.9.15–16) (European Pharmacopoeia, 2017). These experiments were carried out six times; mean values ± SD are reported.

2.6.2. Uptake measurements

Plastic cylinder containers (1 cm of diameter) loaded with 50 mg of CH-AA-BZ_w were subjected to water or SGS sorption (uptake) kinetics using an Enslin's apparatus as described by Nogami et al. (1969) at a room-controlled temperature. The volume of liquid captured by capillarity at pre-established time intervals was measured. All assays were performed in triplicate and the fluid uptake was expressed in mL.

2.7. Release of benznidazole from interpolyelectrolyte complexes

The BZ released from hard gelatin capsules (size 0) containing the multiparticulated IPECs in proportion equivalent to 100 mg of BZ was evaluated. The release rate of BZ from them was measured in a rotating-basket dissolution apparatus (Sotax®AT 7 Smart, Switzerland) at 100 rpm and 37.0 ± 0.5 °C using 900 mL of degassed dissolution medium for distilled water and physiological solution media and the "A" method encoded at the United States Pharmacopoeia (U.S. Pharmacopoeial Convention, 2015) to evaluate modified release dosage forms, which involves the evaluation of the release of BZ in acid medium for 2 h (HCl 0.1 M, 250 mL), followed by a simulated intestinal solution without enzymes for 4 h (phosphate buffer to achieve a final pH 6.8, 750 mL) to simulate gastrointestinal tract conditions was employed. The basket apparatus was selected to avoid floating of the capsules in the dissolution vessel. Standard baskets of 40# mesh size were used. Before each sampling time, 10 mL of medium was taken out of the vessel, filtered through a Teflon® membrane (10 μm pore size) and then returned to the vessel in order to saturate the filter. Finally, samples of 5 mL were taken at defined time intervals, filtered through a Teflon® membrane and replaced with equivalent amounts of preheated fresh medium. BZ released was spectrophotometrically determined at 324 nm (UV–Vis Evolution 300 spectrophotometer, Thermo Electron Corporation, USA).

To evaluate the influence of the sizes particles in the release profiles of BZ, all the fraction collected were analyzed for the CH-AA-BZ_w. The release assays were performed according to "A" method encoded at the United States Pharmacopoeia (U.S. Pharmacopoeial Convention, 2015).

The results are presented as the cumulative percentage of BZ released as a function of time. All of the experiments were conducted in

triplicate; mean values ± SD are reported.

The mean release profiles obtained in water and physiological solution were fitted according to following equations (Eqs. (4) and (5)) (Costa and Lobo, 2001; Siepmann and Peppas, 2001).

The Higuchi model describes drug release as a diffusion process based in the Fick's law. Eq. (4) is generally known as the simplified Higuchi model:

$$\frac{M_t}{M_0} = k_H \times t^{0.5} \tag{4}$$

where "M_t" is the amount of drug permeated at time "t", "M_0" is the initial amount of drug in the donor compartment and "k_H" is a constant reflecting structural and geometric characteristic of the device. In the application of Eq. (4), an independent value, "b", can be obtained, which corresponds to the "*burst effect*" or lag time. From linear analysis of the release profiles, plotting percentage of BZ release with respect to the square root of time, k_H was calculated and the correlation coefficients were determined (R^2).

Eq. (5) proposed by Peppas allows the exponential drug release to be related to the elapsed time; this can be used to characterize different release mechanisms (Peppas, 1985):

$$\frac{M_t}{M_0} = k_P \times t^n \tag{5}$$

where "M_t", "t", "M_0" and "k_P" were described above, and n is the release exponent characterizing the diffusional mechanism. For a slab, when n is 0.5, the fraction of drug released is proportional to the square root of time and the drug release is pure diffusion controlled; when n is 1, drug release is swelling controlled (zero order release kinetics or case-II transport). Values of n between 0.5 and 1 indicate anomalous transport and a superposition of both phenomena. This equation is valid in the release interval between 5 and 60% of the cumulated drug released. Plots of ln M_t/M_0 versus ln t were drawn, n and k_P values were calculated from the slopes and intercepts of the lines, respectively.

The correlation coefficient values (R^2) was used to compare the fit of the profiles using these kinetic models.

In addition, the release profiles of BZ from the multiparticulated IPECs were statistically compared using the similarity factor (f_2, Eq. (6)). According to this methodology, two profiles were considered similar when the f_2 value calculated between them was equal to or greater than 50 (Costa and Lobo, 2001; Food and Drug Administration, 1997).

$$f_2 = 50 \cdot \log\left\{\left(1 + \left(\frac{1}{n}\right)\sum_{t=1}^{n}(R_t - P_t)^2\right)^{-0,5} \cdot 100\right\} \tag{6}$$

Where log is the logarithm to base 10, n is the number of sampling time points, Σ is the summation of all time points and R_t and P_t are the cumulative percentages of drugs released at each of the n time points of the reference and test product, respectively

2.7.1. In vitro mucoadhesion assay

The bioadhesion assay was performed by the mucin particle method (García et al., 2017; Takeuchi et al., 2005) in order to investigate mucin interaction with the IPECs in comparison to their precursors for all (BZ and biopolymers). In this study, pig gastric mucin was used. The mucin was suspended in USP phosphate buffer solution pH 7.4 at a concentration of 0.1 mg mL^{-1} and 3 mL of this suspension was placed in contact with (40 ± 2) mg of each solid at room temperature. After incubation for 48 h, the zeta potentials of mucin suspension in the absence of solids, and mucin suspension in contact with all the solids evaluated were measured in a Zetasizer Nano Series (Malvern®) and change values of the mucin particles due to the presence of the IPECs, BZ or biopolymers was an indication of mucoadhesion (García et al., 2017).

Table 1
Percentages recovered for each fraction of sizes of multiparticulated inter-polyelectrolyte complexes.

Sample	Fraction collected (%)		
	1000–850 μm	850–600 μm	≤600 μm
CH-AA-BZ$_w$	33.82	37.12	29.06
CH-AA-BZ$_h$	67.87	22.36	9.77

2.7.2. Statistical analysis

Statistical significance of comparisons of mean values was assessed by a two-tailed Student's t-test and, two-way ANOVA followed by Tukey's post-test using GraphPad software. A p-value < 0.05 was considered significant.

3. Results

The polysaccharides-based IPECs loaded with BZ were developed using a two-step manufacturing process. First, the casting solvent method was used to obtain BZ-loaded IPEC materials in solid state, using two different interaction media, water or hydroalcoholic solvent. In the second step, wet granulation of the IPEC materials was performed, using water as the wetting agent, to obtain the multiparticles. The mass recovery for multiparticulated products was determined by weight of the dry particles with respect to the initial total amount of solids used, and showed 94 ± 3% w/w of process yield. The wet granulation process allowed us to obtain particles with different sizes. The fractions collected (Retsch GmbH, 2017), presented as percentages recovered, are shown in Table 1.

As can be seen in Table 1, the highest percentage of multiparticles recovered was obtained in the fractions 850–1000 μm and 600–850 μm.

3.1. Physicochemical characterization of IPECs loaded with BZ

Fig. 1 shows images of the multiparticles from both BZ-loaded IPECs (obtained in water and hydroalcohol mixture as interaction media, represented in the left and the right of each image, respectively). The macroscopic images of the multiparticles show that they appear as a pale yellow color with a smooth or slightly porous surface.

The confocal reflection microscopy allowed observation of the superficial microscopic morphological features of the smallest multiparticles (≤600 μm fractions). As can be seen in Fig. 1, the multiparticles based on CH-AA-BZ possess an irregular shape, rough surface, and a heterogeneous coloration. In some regions, orange-brown dyes were observed, while in others, the coloration was pale yellow; this could be related to the natural polysaccharide biopolymers of the IPEC. The interaction media influenced the surface characteristics of the particles. When water was used to obtain the IPEC, BZ was more freely present on the surface of the particles, which is evident by the increased reflection due to its crystallinity. Also, when the interaction medium was a hydroalcoholic mixture, the reflection was lower, which indicates that a higher proportion of BZ was incorporated into the biopolymeric matrix of the particulated system.

The PXRD of the IPECs, PE, BZ, and PM was performed. The PXRD profiles of BZ are shown in Fig. 2. BZ raw material presented a diffraction pattern revealing the characteristic peaks of the crystalline form I of BZ at 19.5°, 23.8°, 24.6° and 25.6° 2Θ/Θ, in accordance with a previous report (Honorato et al., 2014). As can be seen, the characteristics peaks of BZ were also observed in the PXRD patterns of the IPECs obtained in both interaction media; however, they show less intensity than the PM, indicating that a proportion of BZ interact with the polymer matrix and other proportion remains as free crystalline drug even after application of the procedure to obtain the multiparticulated IPECs. No noticeable differences were observed between the PXRD patterns of the IPECs obtained in water and hydroalcoholic

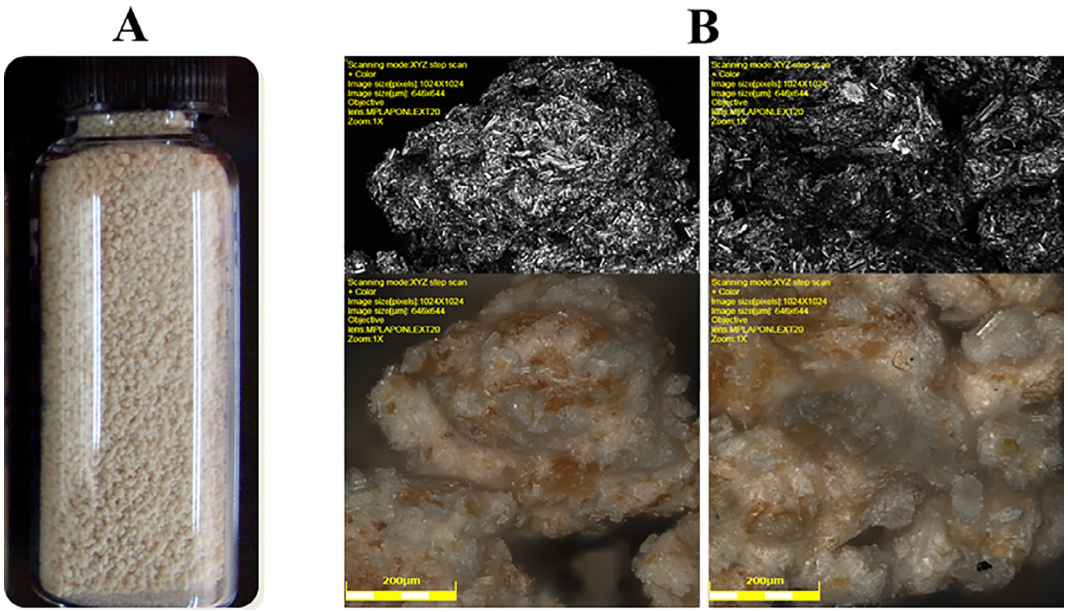

Fig. 1. A) Images of the BZ-loaded IPEC obtained in water as the interaction medium. **B)** Images of the IPECs obtained using water (left images) and hydroalcoholic mixture (right images) as the interaction media, obtained by confocal reflection microscopy (scale bar: 200 µm).

media.

The samples were analyzed by FT-IR and some differences in the band patterns were observed. BZ displayed an amide II band in the region of 1555–1536 cm^{-1}, attributable to an interaction between the N-H bending and the C-N stretching of the C-N-H group. A second, weaker band near 1250 cm^{-1} also resulted from an interaction between the N-H bending and C-N stretching. In addition, carbonyl stretching vibration (amide I band) was observed at 1658 cm^{-1} (Fig. 3). The characteristic bands of BZ were more defined in the spectra corresponding to the PM than both IPECs characterized by different relative intensity, corresponding to the carbonyls groups of BZ and biopolymers. These different patterns observed between both IPEC could be related to the formation of hydrogen bonds between carbonyl groups of the biopolymers and amide groups of BZ. This interaction was less evident in PM.

The spectra of CH-AA-BZ showed different patterns in the region corresponding to the vibration bands of C═O and C–O bonds. Hydroxyl groups of alcohols of CH and AA absorbed strongly at 3450 and 3360 cm^{-1}, respectively (Fig. 3). These bands were shifted to a higher frequency in the spectra of the IPECs, compared to the band patterns of the PM. In addition, the C–O stretching bands of alcohols present in CH and AA, which involve coupling with other vibrations within the molecule, appear between 1030 and 1080 cm^{-1}. The relative intensity of these bands was clearly different in the samples obtained from water compared to those obtained in hydroalcoholic media (Fig. 3). These findings could all be due to the formation of hydrogen bonds between hydroxyl groups of the biopolymers and the carbonyl group of BZ, which is observed in the two IPECs. The spectra of AA shows the characteristic bands, and highlights the band corresponding to the carbonyl group (C═O) stretching vibration at higher frequencies (approx. 1730 cm^{-1}). This band was more intense in the two IPECs than in the PM; this could be due to ionic interaction between the two PE.

Fig. 4 shows the DSC and TGA curves of each IPEC, their precursors (AA, CH, BZ,), and the PM (CH-AA-BZ). DSC curves shown in Fig. 4A correspond to a second heating run in which the moisture of samples was previously eliminated by an isotherm at 100 °C for 10 min.

The DSC curve of BZ presents an intense endothermic peak (onset: 190.4 °C, maximum peak: 191.2 °C) without mass loss in TGA, corresponding to the melting point of the crystalline form. In the assay conditions, neither moisture nor drug decomposition of BZ was detectable. In assayed conditions, the events corresponding to glass transition (*Tg)* of pure PE were not present, since reported *Tg* values for AA and CH are ~110 °C and ~200 °C, respectively (Dong et al., 2004; Sakurai et al., 2000). The DSC curve of the PM showed a similar endothermic peak corresponding to the melting point of pure BZ.

In the DSC curves for both IPECs, the melting process of BZ showed a small and wide endothermic peak which is substantially lower than expected for the amount of BZ in the sample, followed by an exothermic event above 195 °C, attributable to a decomposition process. In addition, a shift of baseline at 157 °C, which it is not present in the DSC curve of PM, may be attributed to glass transition of CH-BZ-AA complexes.

The TGA curves presented in Fig. 4B suggest that, under heating, AA and CH initially underwent a dehydration process between 70 and 100 °C, with mass loss of 4–5%, followed by decomposition above 170 °C and 280 °C for AA and CH, respectively. The TGA curve of BZ proved the anhydrous conditions of this crystalline drug, and only a decomposition process above 210 °C was observed. Both IPECs and the PM showed similar TG curves; however, both IPECs presented a higher weight loss than PM, which could be attributable to a wet granulation process.

3.2. Flow properties of BZ-loaded multiparticulated IPECs

Table 2 shows the flow properties of BZ and the multiparticles corresponding to the highest fraction collected (850–1000 µm). As expected, the multiparticles demonstrated significantly improved flow properties, compared to those of powdered pure BZ, which are adequate for the production of monolithic solid dosage forms (capsules). In fact, according to European Pharmacopeia scores, the Carr's Index and the Hausner's ratio of BZ changed in the IPECs from very poor to excellent flow properties, and the angle of repose changed from poor to acceptable (Staniforth, 2002) depending on the IPEC. There were no observed differences between the IPEC obtained in water and that obtained in hydroalcoholic mixture as the interaction media.

3.3. Fluid uptake by BZ-loaded IPECs

Water and SGS sorption were evaluated to assess the uptake of fluids by the IPEC multiparticles obtained in water as the interaction medium.

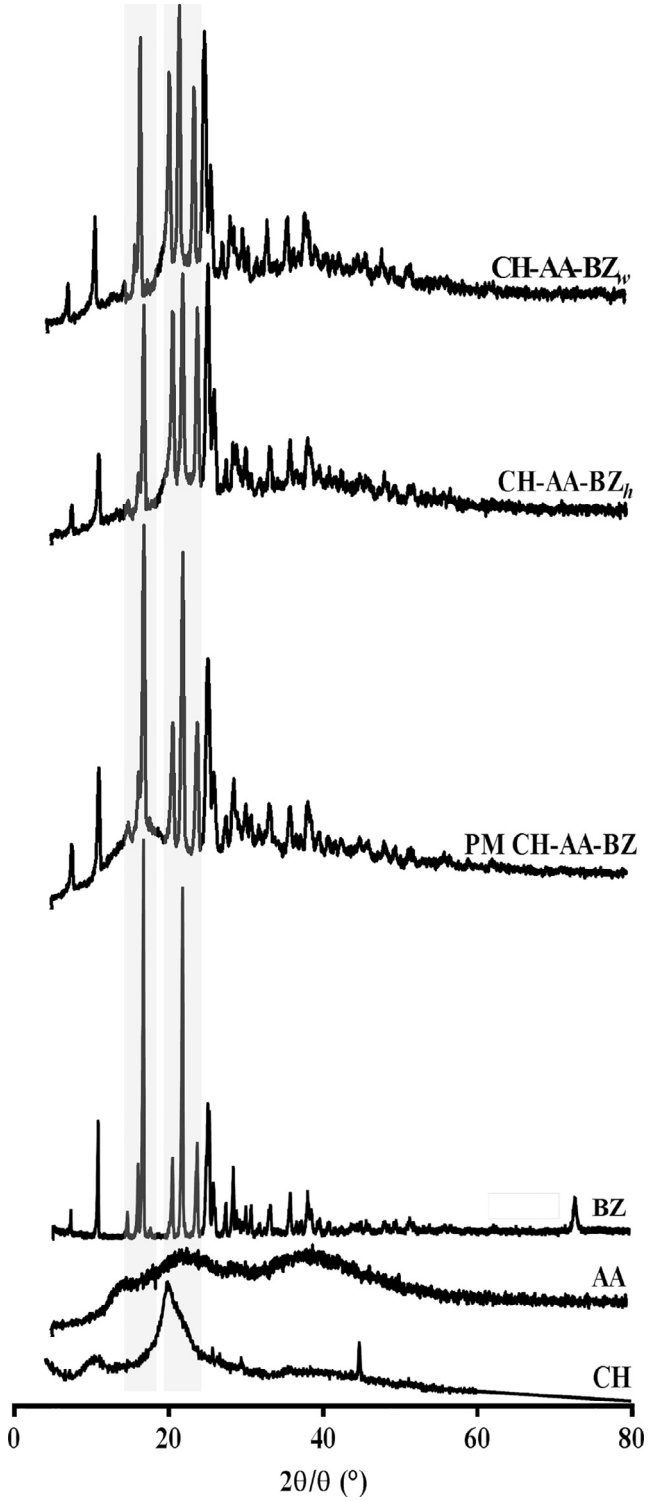

Fig. 2. Powder X-ray diffraction patterns of both the IPEC obtained in water and the IPEC obtained in the hydroalcoholic mixture, their precursors, and the physical mixture (PM CH-AA-BZ).

An Enslin's apparatus was used, which allows measurement of the volume of liquid captured by capillarity at pre-established time intervals. Fig. 5A shows the water and SGS uptakes, respectively, at room temperature, as a function of time (min). The water uptake of CH-AA-BZ_w showed a very fast capture of 0.2 mL of fluid (corresponding to 400% w/w), followed of a linear sorption of water as a function of time. Similar results were observed for the uptake of SGS, but in this case, the initial amount of fluid uptake was 0.5 mL (corresponding to 1000% w/w). In assay conditions, the total amount of fluids captured for this system over 180 min was higher in SGS (1.2 mL) in comparison to water (0.85 mL) (corresponding to 2400% and 1700% of incremental weight, respectively).

The sorption rates of fluids determined from the linear regression of the uptake profiles are presented in the legend of Fig. 5. These results revealed that the linear regressions for the sorption profiles were adequate, given that the R^2 was higher than 0.97 in both profiles evaluated.

Fig. 5B shows the macroscopic aspect of the multiparticles of CH-AA-BZ_w at 0, 90, and 180 min during the assay of water uptake, corresponding to the initial condition, midpoint of the assay, and final evaluation time, respectively. These images illustrate that most of the particles contained in the hollow cylinder are wetted with SGS. CH-AA-BZ_w developed a broad gel layer and exhibited remarkable swelling. The particles had a similar appearance when the sorption medium was water.

3.4. Drug release behavior of BZ-loaded IPECs

The BZ release behaviors from the IPECs were studied to evaluate their performance as an oral drug delivery dosage form. Water and saline solution were used as simple models of physiological fluids to evaluate the main kinetic mechanisms involved in the release of BZ from both IPEC. In addition, a specific pharmacopoeia method, to evaluate modified release dosage forms, which simulates gastrointestinal tract conditions (gastric followed by intestinal environment) was used. Fig. 6A shows the BZ release profiles from CH-AA-BZ_w to water and physiological solution. A slow and extended release of BZ towards both receptor media was observed. However, a massive release of BZ during the first 30 min, and important "*burst*" effects were present in both release media; approximately 20 and 40% of BZ was released during the first 5 min, in saline solution and water, respectively. In assay conditions, after the first hour, both release profiles showed a controlled and sustained release of BZ, and the drug loaded in the IPEC was completely released in water after 6 h, while only 50% of BZ was released toward saline solution at the same time point. Thus, the release media influenced the release of BZ, and different release profiles from each complex was obtained (f_2 = 24.5).

Kinetic analysis of *in vitro* release data using Higuchi and Peppas equations was performed in order to evaluate the main mechanism of BZ transport through the biopolymeric matrix of the IPEC both toward water and physiological solution. This data is summarized in Table 3. The BZ release profiles of multiparticles from CH-AA-BZ_w, plotted as Higuchi and Peppas model, in physiological solution, were found to be linear for both models. Regression coefficient values (R^2 = 0.99) were higher for physiological solution, compared to those obtained in water (R^2 = 0.95). The BZ release from the CH-AA-BZ_w complex was characterized by a diffusional process; the swelling of microparticles may be the main mechanism of kinetics control in both assayed conditions.

Fig. 6B shows the release profiles of BZ from both IPEC, using a specific pharmacopoeia method to evaluate modified release dosage forms, which simulates gastrointestinal tract conditions. As can be seen, for both IPECs, an initial "burst effect" for both IPECs, reaching up to 10% of BZ released in the first 5 min was observed. After that, the release of BZ was modulated; approximately 55 and 65% of BZ was released during the first 2 h (acid stage), from CH-AA-BZ_h and CH-AA-BZ_w, respectively. The interaction medium (water or hydroalcoholic mixture) used to obtain the IPECs did not influence the release of BZ, and similar release profiles were obtained from both complexes (f_2 = 53.08).

Furthermore, the kinetic data for both the IPEC obtained in water and the IPEC obtained in hydroalcoholic mixture was analyzed (Table 3); only the simulated gastric environment was considered in these analyses. The release data of BZ from CH-AA-BZ_h, plotted as Higuchi and Peppas model, was found to be linear for each IPEC, which is

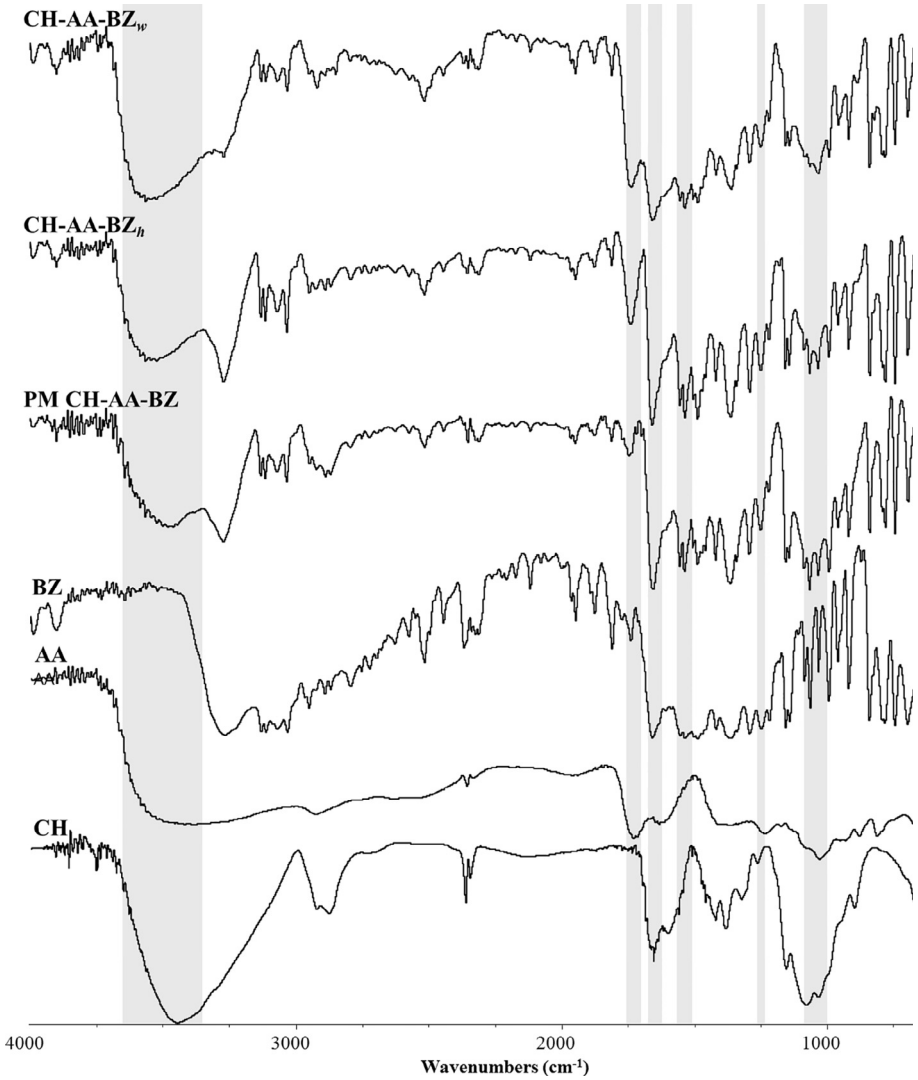

Fig. 3. FT-IR spectra of both the IPEC obtained in water and the IPEC obtained in hydroalcoholic mixture, their precursors, and the physical mixture (PM CH-AA-BZ).

supported by their regression coefficient values ($R^2 = 0.98$). The drug transport mechanism of BZ from CH-AA-BZ$_h$ was found to be anomalous (non-Fickian) diffusion, as determined by an n value > 0.45 and < 0.89 (Costa and Lobo, 2001). However, from CH-AA-BZ$_w$, the release of BZ showed a lower fit in the kinetic models evaluated, evidenced by low R^2 values (0.94 and 0.88 for Higuchi and Peppas models, respectively). In terms of R^2 values, CH-AA-BZ$_w$ had the best fit with the Higuchi release model, in which drug diffusion across swelled particles would be the preponderant mechanism of BZ delivery.

The analysis of the influence of particle sizes on the release profiles of BZ was performed for CH-AA-BZ$_h$ (Fig. 6C). The release rates of BZ were slightly higher at lower particle sizes. In addition, the pH-sensitive property of the IPEC toward the release media, assayed after 2 h, was more evident at lower particle sizes. This finding is in accordance with the anomalous kinetic behavior, in which both IPEC relaxation and diffusion process take place.

3.5. In vitro mucoadhesion

The *in vitro* interaction of IPEC multiparticles, and their precursors, with mucin was characterized by measuring the zeta potential of mucin suspension under equilibrium conditions. Mucin in aqueous dispersion was used as a control in this assay. Fig. 7 shows the zeta potential under the different conditions evaluated. As can be seen, mucin possessed a negative charge due to ionization of carboxyl groups, since environmental pH was higher than its pKa (pKa of mucin = 2.6). In the presence of the IPECs, and their precursors, the zeta potential of mucin changed to higher negative values ($^{****}p < 0.001$ and $^{**}p < 0.01$, Fig. 7). Further, a significant difference ($^{**}p < 0.01$) was observed between the IPEC obtained in water (CH-AA-BZ$_w$) and the IPEC obtained in hydroalcoholic mixture (CH-AA-BZ$_h$) as interaction media; however, both of these IPECs were significantly different from pure mucin.

4. Discussion

In this study, we provide new knowledge related to BZ-loaded polysaccharides-based pharmaceutical technology approaches aimed to improve Chagas disease pharmacotherapy. Specifically, we report on a strategy involving mucoadhesive and biocompatible multiparticulated systems for controlled BZ release.

The use of multiparticles for oral drug delivery offers numerous advantages over single-unit dosage forms, namely multiplicity and small sizes, more uniform and reliable gastrointestinal transit, low risk of dose dumping, reduction in risk of systemic toxicity, and reduced incidence of side effects (AlHusban et al., 2011; Auriemma et al., 2013; Dey et al., 2008; Pan et al., 2010; Severino et al., 2012).

To study the polysaccharides-based systems that we developed, the

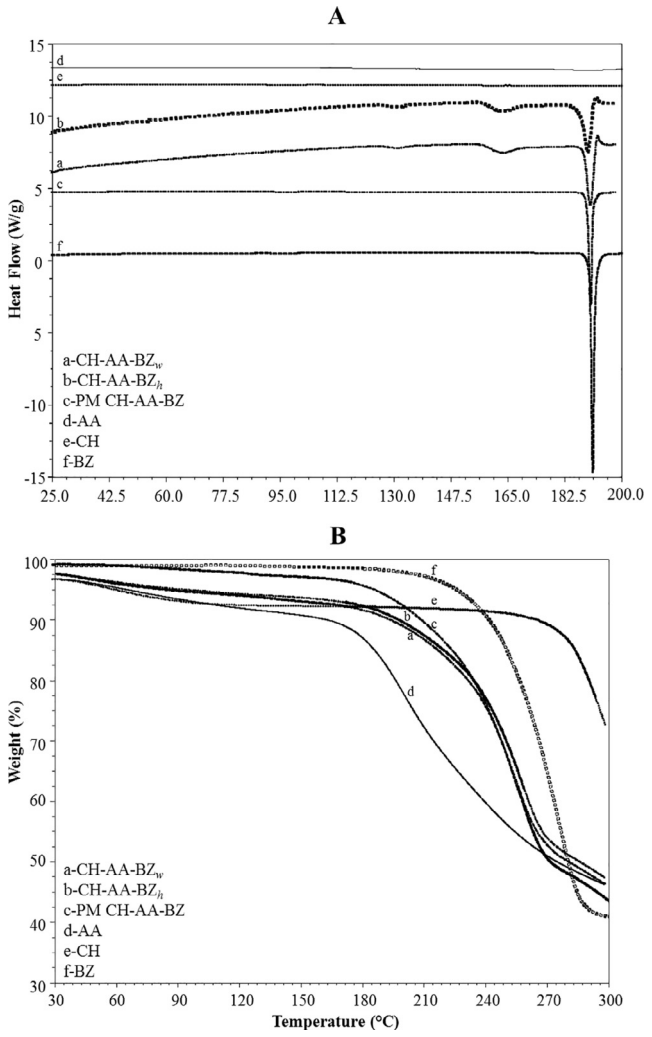

Fig. 4. A) DSC and **B)** TGA curves of both IPECs (CH-AA-BZ), their precursors, and their physical mixture (PM CH-AA-BZ).

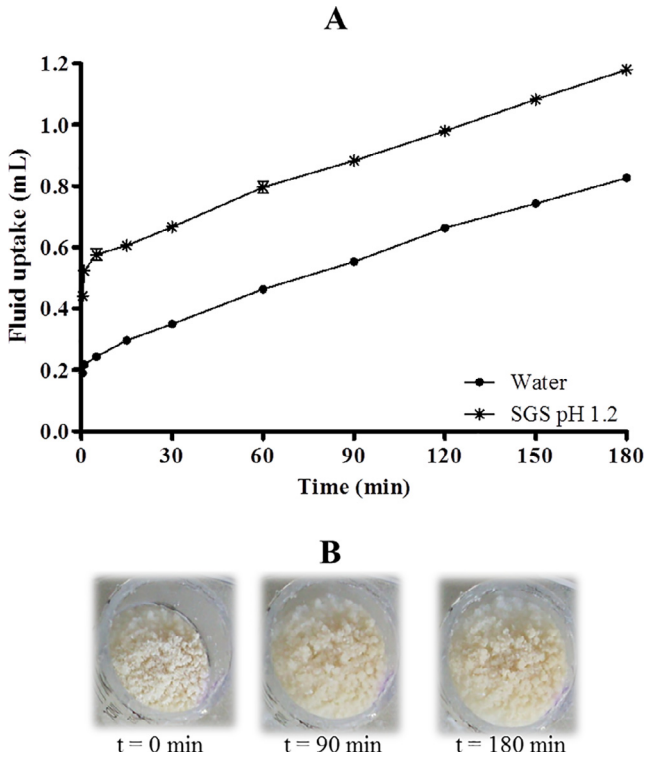

Fig. 5. A) Uptake of water and SGS by 50 mg BZ-loaded IPEC obtained in water as the interaction medium. The sorption rates of water and SGS determined from the linear regression of the uptake profiles for the IPEC multiparticles were 3.47 ± 0.07 μL min^{-1} with $R^2 = 0.99$ and 3.7 ± 0.1 μL min^{-1} with $R^2 = 0.97$, respectively. **B)** Images of the IPEC based on CH-AA-BZ$_w$ at different times of the assays of SGS uptake.

yields for obtaining the multiparticles of BZ-loaded IPECs, with respect to the initial amount of solid (drug and biopolymers) employed, were analyzed. Table 1 shows that yields higher than 91% were obtained for all fractions collected. It is important to stress that the methodologies employed (casting solvent and wet granulation) in order to obtain the BZ-loaded IPEC multiparticles were simple and scalable to higher production. Flow properties of particles were also evaluated (Table 2) and these multiparticles were found to have better flow properties than pure BZ. The Carr's Index and the Hausner's ratio were excellent, and the angle of repose was good, indicating that both multiparticulated BZ-loaded IPECs are adequate for producing monolithic solid dosage forms (capsules) (Vila Jato, 1997).

The macroscopic observation of the polysaccharides-based BZ-loaded IPEC multiparticles (Fig. 1A) showed that they are a pale yellow color, in accordance with the intrinsic color of the biopolymers employed, and have a smooth or slightly porous surface. However, the microscopic observation using confocal reflection microscopy (Fig. 1B) showed that the BZ-loaded IPEC multiparticles possess irregular shapes, rough surfaces, and a heterogeneous coloration, with some regions presenting with orange-brown dyes were evident microscopically despite macroscopic pale yellow observations. Further, the interaction media influenced the surface characteristics of the multiparticles. The IPEC obtained in water as interaction media showed a higher proportion of crystalline BZ as acicular crystals on the surface of the particles, while the IPEC obtained in hydroalcoholic medium had a smaller proportion of free crystalline BZ. This could be attributed to a higher proportion of BZ being incorporated into the biopolymeric matrix, facilitated by its higher solubility in hydroalcoholic mixture than water. These results are in accordance with the PXRD obtained (Fig. 2). It has been reported that binary polyelectrolyte-drug complexes obtained by mixing a polyelectrolyte with an oppositely charged drug, in a convenient medium (water or ethanol) able to dissolve one or both components, result in solid amorphous materials where the drug is ionically

Table 2
Flow properties of particles of BZ and BZ-loaded IPEC.

Sample	Flow parameters				
	Bulk density (g mL^{-1})	Tap density (g mL^{-1})	Carr's Index	Hausner's ratio	Angle of repose (°)
BZ (powder)	0.11 ± 0.01	0.24 ± 0.02	54 ± 2	2.16 ± 0.03	52 ± 2
CH-AA-BZ$_w$	0.33 ± 0.01	0.33 ± 0.03	4 ± 1	1.04 ± 0.01	36 ± 1
CH-AA-BZ$_h$	0.35 ± 0.02	0.34 ± 0.03	3 ± 1	1.03 ± 0.01	37 ± 2

Note: Carr's Index lower than 12% indicates excellent flow for particulated solids and angle of repose lower than 40° indicates acceptable flow properties (Staniforth, 2002).

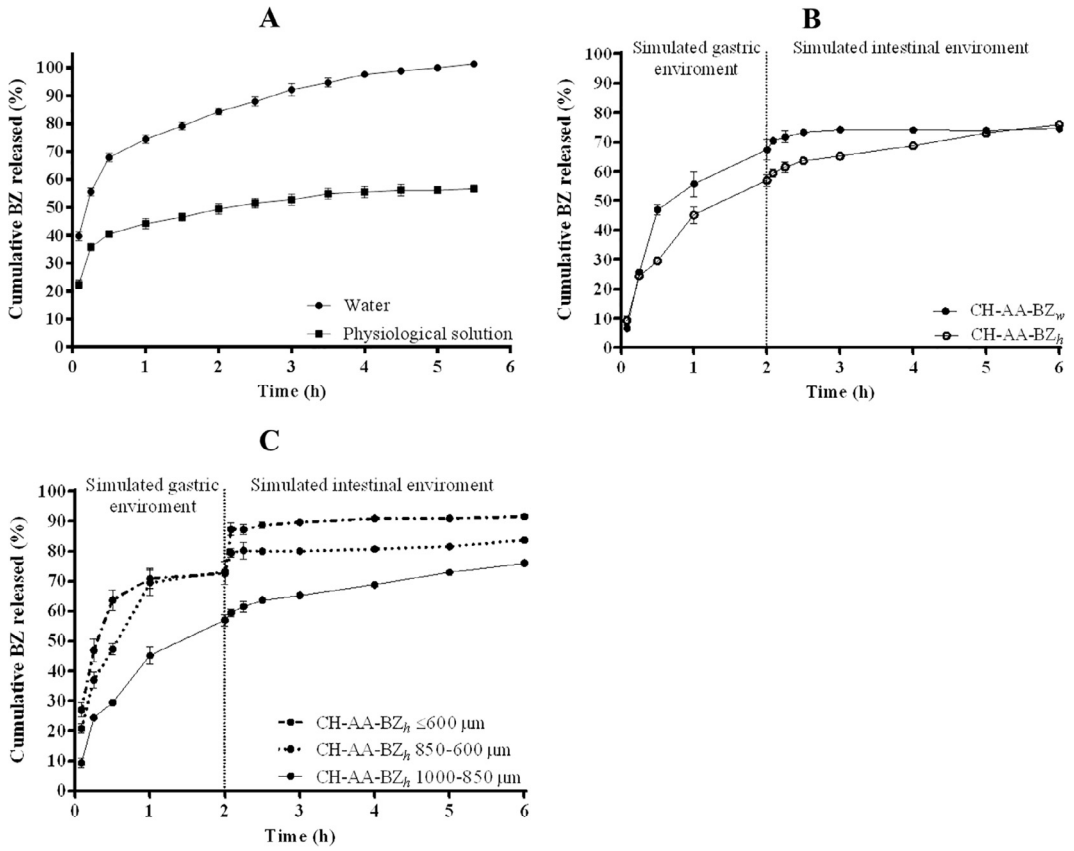

Fig. 6. A) Release profiles of BZ from IPEC obtained in water as the interaction media, towards water and physiological solution. **B**) Release profiles of BZ in method A-USP medium for both the IPEC obtained in water and the IPEC obtained in hydroalcoholic mixture as interaction media. **C)** Release profiles of BZ in method A-USP medium from polysaccharides-based IPEC with different particles sizes (IPEC obtained in hydroalcoholic medium).

bonded to the biopolymeric carrier (Olivera et al., 2017). Further, IPECs loaded with different drugs have been found to exhibit an absence of significant signals in the PXRD, indicating that they have an amorphous state (Moustafine, 2011; Moustafine et al., 2011; Palena et al., 2015). In contrast, BZ-loaded IPECs presented with diffractograms characteristic of crystalline materials, with sharp peaks observed on PXRD (Fig. 2). This could be because BZ does not have ionizable groups in its chemical structure that able to interact with the polyelectrolytes; thus, BZ is molecularly dispersed in the biopolymeric matrix (Huang and Dai, 2014) where the two polyelectrolytes can interact ionically (Moustafine, 2011). Accordingly, evidence of acid-base reactions between CH and AA were observed. Further, the band characteristics of BZ were more defined in the spectra corresponding to the PM than both the IPEC obtained in water and the IPEC obtained in hydroalcoholic media (Fig. 3).

In line with these results, thermal analysis of both IPECs showed that a proportion of BZ remains in a free crystalline form, showing a broad endothermic peak and lower enthalpy at the melt temperature of pure BZ. DSC curves for both IPECs showed a new shift in the baseline at 159 °C that could be attributable to glass transition of CH-AA-BZ complexes.

The applicability of novel biopolymeric matrices as drug carriers can be determined by studying their swelling capacity in relevant media, including those that imitate the passage through the gastrointestinal tract (Moustafine et al., 2011). We studied the water sorption with a simple model and SGS to assess the uptake of fluids by the multiparticulated complex CH-AA-BZ_w using an Enslin's apparatus. Notable differences were observed between the water and SGS uptakes by the BZ-loaded IPEC (Fig. 5). The swelling properties of CH-AA-BZ_w were remarkably higher in SGS compared to water. However, the sorption rates in both swelling media, determined from the linear regression of the uptake profiles, showed values of $0.00347 \pm 0.00007\ mL\ min^{-1}$ and $0.0037 \pm 0.0001\ mL\ min^{-1}$ for water and SGS, respectively, which indicates that the initial fluid uptake, approximately double in SGS in comparison to water, was the main reason for the remarkable differences observed in the sorption capacity of the multiparticles. There were no noticeable differences observed in uptake rates. Related to that, it has been reported that the permeability of a biopolymeric matrix in relation to a drug is strongly dependent on its water content. The mobility of the macromolecules increases at higher relative amounts of water and, thus, the free volume available for diffusion is increased. Thus, the fluid uptake and the consequent swelling of the multiparticles obtained is an important parameter associated with the mechanism and kinetics of active release (Lacerda et al., 2014). Our results suggest that the multiparticles undergo pH-dependent fluid uptake (Fig. 5). A previous study has reported that microparticles of alginate and CH at low pH exhibit swelling due to protonation of the primary amino groups of the CH, and with increasing pH, the swelling of the microparticles increases. In contrast, our IPEC multiparticles exhibited higher uptake of SGS than water. These differences can be attributed at the presence of electrolytes in the solution, given that the swelling studies have been performed in SGS or buffer phosphate solution at pH 6.8. However, our results also revealed that IPEC multiparticles based on ionic complexes between CH and AA act as a pH-dependent polyelectrolyte complex, where the amino and carboxylate groups respond to stimuli from the environment in which they are inserted (Lacerda et al., 2014).

The release of BZ from CH-AA-BZ_w towards water and physiological solution allowed the study of the kinetic mechanisms involved in its release. As can be seen, the release of BZ was modified (Fig. 6A) and significant differences were observed in the release profiles obtained toward water as compared to physiological solution as a receptor

Table 3
Kinetic data obtained from BZ release studies of both the IPEC obtained in water and the IPEC obtained in hydroalcoholic mixture toward the simulated gastric environment (method A-USP), using Higuchi and Peppas equations.

IPEC	Release media	Higuchi			Peppas		
		k_H (%.$h^{-0.5}$)	b^* (%)	R^2	k_P (%.h^{-n})	n	R^2
CH-AA-BZ_w	*Water*	29.2	44.0	0.95	33.7	0.47	0.95
CH-AA-BZ_w	*Physiological solution*	13.3	30.4	0.99	21.5	0.30	0.99
CH-AA-BZ_w	*Simulated gastric environment*	29.4	0.0	0.94	46.7	0.53	0.88
CH-AA-BZ_h		21.0	13.2	0.98	32.9	0.58	0.98

* *b*: value corresponding to the intersection of the extrapolated line with the y axis.

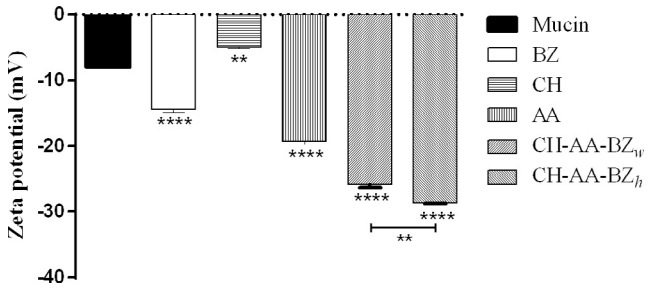

Fig. 7. Interactions between mucin and the IPECs (CH-AA-BZ_w and CH-AA-Bz_h), and their precursors (CH, AA, and BZ), measured with dynamic light scattering. Asterisks indicate a significant difference between the indicated groups with respect to mucin ($^{****}p < 0.001$ and $^{**}p < 0.01$); the line denotes a significant difference between the IPECs obtained in the different media.

medium ($f_2 = 24.5$). Further, Fickian transport with a preponderant release mechanism controlled by drug diffusion was observed (Table 3), which is in agreement with the analysis using Higuchi and Peppas kinetic models (Costa and Lobo, 2001; Siepmann and Peppas, 2001).

Regarding the release of BZ from both multiparticulated IPECs towards the fluids which simulate gastrointestinal tract conditions (Fig. 6B), we observed a modulated release of BZ; up to 65% of BZ was released in the gastric environment, and there was no influence of the interaction media for obtaining the IPEC ($f_2 = 53.08$). Furthermore, the analysis of BZ release from CH-AA-BZ_w showed a poor plot (low correlation coefficients). In terms of R^2, the drug transport mechanism was found to be Fickian diffusion, and in accordance with the swelling results, BZ diffusion across to swelled particles is the preponderant mechanism of kinetic control. However, BZ delivery from CH-AA-BZ_h showed a shift in the kinetic control, and the release profile presented anomalous behavior, in which BZ transport is determined by both drug diffusion and IPEC relaxation in the dissolution medium (Costa and Lobo, 2001; Siepmann and Peppas, 2001). In line with this result, the amount of BZ released from CH-AA-BZ_h (Fig. 6C) was slightly higher at lower particle sizes, which could be related to the gel layer erosion of swelled particles. In addition, this system showed an increase in the pH-sensitive property at lower particles sizes, which is also related to the larger surface exposed for the erosion in the acid release media. The anomalous kinetic behavior can be explained considering that besides IPEC relaxation in the dissolution medium (Costa and Lobo, 2001; Siepmann and Peppas, 2001), the diffusion process has great influence in the drug release. If each particle is considered as a sphere, when the particle size is decreased, the larger surface area of the particle allows the increase in the surface area to volume ratio, thus increasing the surface area in contact with the release media, which increases the dissolution rate of the drug (Khadka et al., 2014).

Mucoadhesion is an important property because it provides many advantages, which include increased residence time at application sites (in this case, in the gastrointestinal tract), increased drug permeation, and improved drug availability (Bassi da Silva et al., 2017). All of these benefits allow improvement in the performance of the BZ-loaded IPECs. Our results (Fig. 7) showed significant changes in the zeta potential values which are evidence that interactions occur between the solids and mucin; this reveals the bioadhesive properties of the multiparticles of the BZ-loaded IPECs obtained in both interaction media (García et al., 2017).

Considering the results as a whole, it is possible to establish that the flow properties of the BZ-loaded IPECs obtained in both interaction media showed suitable flowability features for hard gelatin-capsule formulation. The multiparticulated BZ-loaded IPECs exhibited mucoadhesion properties, and the release profiles revealed modulation of BZ release, depending on the release media, in accordance with the fluid uptake. Thus, the BZ-loaded IPECs act as a reservoir for the drug, and these systems can be used to design bioadhesive and controlled BZ delivery systems.

5. Conclusions

Multiparticulated BZ-loaded IPECs were obtained and their physicochemical and pharmacotechnical properties were evaluated. The mucoadhesive behavior and controlled BZ release are encouraging characteristics for the design of novel therapeutic alternatives to improve the treatment of Chagas disease, which could diminish BZ adverse effects and/or allow a reduction in the frequency of its administration.

Funding information

This work was supported by Agencia Nacional de Promoción Científica y Tecnológica – Fondo para la Investigación Científica y Tecnológica, Argentina (Grant No. FONCyT-program, PICT 2012-0173); Consejo Nacional de Investigaciones Científicas y Técnicas, Argentina (Grant No.: CONICET, PIP 2013–2016, N°: 11220120100461); Secretaría de Ciencia y Tecnología. Universidad Nacional de Córdoba, Argentina (Grant No.: SECYT-UNC, 2014–2016, N°: 30720130100922CB).

Acknowledgements

Manzo RH and Jimenez-Kairuz AF are members of CONICET scientific career. García MC, thanks to CONICET for postdoctoral fellowship.

Authors thank Mgter. Norma Maggia (Lab. of Thermal Analysis, UNITEFA, CONICET-UNC) for technical assistance and perform of DSC-TGA runs. Authors also thank Dra. Marisa Martinelli (Instituto de Investigación y Desarrollo en Ingeniería de Procesos y Química Aplicada (IPQA), CONICET- UNC) for her help in the analysis of the FT-IR spectra. Furthermore, authors would like to thank Coordinación Nacional de Control de Vectores and Ministerio de Salud de la Nación (filial Córdoba) for supplying the Radanil® tablets used to do this work.

Special thank at the professional editing and proofreading of this document made by Proof-Reading-Service.com, ensuring consistency of the spelling, grammar and punctuation.

References

Ahmed, T.A., Aljaeid, B.M., 2016. Preparation, characterization, and potential application of chitosan, chitosan derivatives, and chitosan metal nanoparticles in pharmaceutical drug delivery. Drug Des. Dev. Therapy 10, 483.

Algul, D., Sipahi, H., Aydin, A., Kelleci, F., Ozdatli, S., Yener, F.G., 2015. Biocompatibility of biomimetic multilayered alginate–chitosan/β-TCP scaffold for osteochondral tissue. Int. J. Biol. Macromol. 79, 363–369.

AlHusban, F., Perrie, Y., Mohammed, A.R., 2011. Formulation of multiparticulate systems as lyophilised orally disintegrating tablets. Eur. J. Pharm. Biopharm. 79, 627–634.

Auriemma, G., Mencherini, T., Russo, P., Stigliani, M., Aquino, R.P., Del Gaudio, P., 2013. Prilling for the development of multi-particulate colon drug delivery systems: pectin vs. pectin–alginate beads. Carbohydr. Polym. 92, 367–373.

Bani-Jaber, A., Al-Aani, L., Alkhatib, H., Al-Khalidi, B., 2011. Prolonged intragastric drug delivery mediated by Eudragit® E-Carrageenan polyelectrolyte matrix tablets. AAPS PharmSciTech 12, 354–361.

Bani-Jaberm, A.K., Alkawareek, M.Y., Al-Gousous, J.J., Abu Helwa, A.Y., 2011. Floating and sustained-release characteristics of effervescent tablets prepared with a mixed matrix of Eudragit L-100-55 and Eudragit E PO. Chem. Pharm. Bull. 59, 155–160.

Bassi da Silva, J., Ferreira, de Freitas, S.B.d.S.O., Bruschi, M.L., 2017. A critical review about methodologies for the analysis of mucoadhesive properties of drug delivery systems. Drug Dev. Ind. Pharm. 43, 1053–1070.

Bellera, C., Sbaraglini, M., Balcazar, D., Fraccaroli, L., Cristina Vanrell, M., Florencia Casassa, A., Labriola, C., Romano, P., Carrillo, C., Talevi, A., 2015. High-throughput drug repositioning for the discovery of new treatments for Chagas disease. Mini Rev. Med. Chem. 15, 182–193.

Bermudez, J., Davies, C., Simonazzi, A., Real, J.P., Palma, S., 2016. Current drug therapy and pharmaceutical challenges for Chagas disease. Acta tropica 156, 1–16.

Cencig, S., Coltel, N., Truyens, C., Carlier, Y., 2012. Evaluation of benznidazole treatment combined with nifurtimox, posaconazole or Am Bisome(R) in mice infected with *Trypanosoma cruzi* strains. Int. J. Antimicrob. Agents 40, 527–532.

Costa, P., Lobo, J.M.S., 2001. Modeling and comparison of dissolution profiles. Eur. J. Pharm. Sci. 13, 123–133.

Chatelain, E., Ioset, J., 2011. Drug discovery and development for neglected diseases: the DNDi model. Drug Des. Dev. Therapy 5, 175–181.

Davies, C., Dey, N., Negrette, O., Parada, L., Basombrio, M., Garg, N., 2014. Hepatotoxicity in mice of a novel anti-parasite drug candidate hydroxymethylnitrofurazone: a comparison with Benznidazole. PLoS Negl. Trop. Dis. 8, 1–12.

de Melo, P.N., Barbosa, E.G., Garnero, C., de Caland, L.B., Fernandes-Pedrosa, M.F., Longhi, M.R., da Silva-Júnior, A.A., 2016. Interaction pathways of specific co-solvents with hydroxypropyl-β-cyclodextrin inclusion complexes with benznidazole in liquid and solid phase. J. Mol. Liq. 223, 350–359.

Dey, N., Majumdar, S., Rao, M., 2008. Multiparticulate drug delivery systems for controlled release. Trop. J. Pharm. Res. 7, 1067–1075.

Dong, Y., Ruan, Y., Wang, H., Zhao, Y., Bi, D., 2004. Studies on glass transition temperature of chitosan with four techniques. J. Appl. Polym. Sci. 93, 1553–1558.

European Pharmacopoeia, P.E., 2017. European Pharmacopoeia 8th ed. European Directorate for the Quality of Medicines & HealthCare, Council of Europe 7 allée Kastner, CS 30026.

Fonseca-Berzal, C., Palmeiro-Roldán, R., Escario, J.A., Torrado, S., Arán, V.J., Torrado-Santiago, S., Gómez-Barrio, A., 2015. Novel solid dispersions of benznidazole: preparation, dissolution profile and biological evaluation as alternative antichagasic drug delivery system. Exp. Parasitology 149, 84–91.

Food and Drug Administration, F., 1997. Guidance for Industry: Dissolution testing of immediate-release solid oral dosage forms, Food and Drug Administration. Center for Drug Evaluation and Research (CDER).

García, M., Manzo, R., Jimenez-Kairuz, A., 2015. Extemporaneous benznidazole oral suspension prepared from commercially available tablets for treatment of Chagas disease in paediatric patients. Trop. Med. Int. Health 20 (7), 864–870.

García, M.C., Aldana, A.A., Tártara, L.I., Alovero, F., Strumia, M.C., Manzo, R.H., Martinelli, M., Jimenez-Kairuz, A.F., 2017. Bioadhesive and biocompatible films as wound dressing materials based on a novel dendronized chitosan loaded with ciprofloxacin. Carbohydr. Polym. 175, 75–86.

García, M.C., Ponce, N.E., Sanmarco, L.M., Manzo, R.H., Jimenez-Kairuz, A.F., Aoki, M.P., 2016. Clomipramine and Benznidazole act synergistically and ameliorate the outcome of experimental Chagas disease. Antimicrob. Agents Chemother. 60, 3700–3708.

Honorato, S.B., Mendonça, J.S., Boechat, N., Oliveira, A.C., Mendes Filho, J., Ellena, J., Ayala, A.P., 2014. Novel polymorphs of the anti-*Trypanosoma cruzi* drug benznidazole. Spectrochim. Acta Part A Mol. Biomol. Spectrosc. 118, 389–394.

Huang, Y., Dai, W.-G., 2014. Fundamental aspects of solid dispersion technology for poorly soluble drugs. Acta Pharma. Sin. B 4, 18–25.

Jabeen, S., Kausar, A., Saeed, S., Muhammad, B., Gul, S., Farooq, M., 2016. Crosslinking of alginic acid/chitosan matrices using bis phenol-F-diglycidyl ether: mechanical, thermal and water absorption investigation. Int. J. Plast. Technol. 20, 159–174.

Jeganathan, B., Prakya, V., 2015. Interpolyelectrolyte complexes of Eudragit® EPO with hypromellose acetate succinate and Eudragit® EPO with hypromellose phthalate as potential carriers for oral controlled drug delivery. AAPS PharmSciTech 16, 878–888.

Karbassi, E., Asadinezhad, A., Lehocký, M., Humpolíček, P., Vesel, A., Novák, I., Sáha, P., 2014. Antibacterial performance of alginic acid coating on polyethylene film. Int. J. Mol. Sci. 15, 14684–14696.

Khadka, P., Ro, J., Kim, H., Kim, I., Kim, J.T., Kim, H., Cho, J.M., Yun, G., Lee, J., 2014. Pharmaceutical particle technologies: An approach to improve drug solubility, dissolution and bioavailability. Asian J. Pharm. Sci. 9, 304–316.

Kim, H.-L., Jung, G.-Y., Yoon, J.-H., Han, J.-S., Park, Y.-J., Kim, D.-G., Zhang, M., Kim, D.-J., 2015. Preparation and characterization of nano-sized hydroxyapatite/alginate/chitosan composite scaffolds for bone tissue engineering. Mater. Sci. Eng., C 54, 20–25.

Kong, M., Chen, X.G., Xing, K., Park, H.J., 2010. Antimicrobial properties of chitosan and mode of action: a state of the art review. Int. J. Food Microbiol. 144, 51–63.

Lacerda, L., Parize, A.L., Fávere, V., Laranjeira, M.C.M., Stulzer, H.K., 2014. Development and evaluation of pH-sensitive sodium alginate/chitosan microparticles containing the antituberculosis drug rifampicin. Mater. Sci. Eng., C 39, 161–167.

Leonardi, D., Bombardiere, M.E., Salomon, C.J., 2013. Effects of benznidazole: cyclodextrin complexes on the drug bioavailability upon oral administration to rats. Int. J. Biol. Macromol. 62, 543–548.

Leonardi, D., Salomón, C.J., Lamas, M.C., Olivieri, A.C., 2009. Development of novel formulations for Chagas' disease: optimization of benznidazole chitosan microparticles based on artificial neural networks. Int. J. Pharm. 367, 140–147.

Maximiano, F., de Paula, L., Figueiredo, V., de Andrade, I., Talvani, A., Sa-Barreto, L., Bahia, M., Cunha-Filho, M., 2011. Benznidazole microcrystal preparation by solvent change precipitation and in vivo evaluation in the treatment of Chagas disease. Eur. J. Pharm. Biopharm. 78, 377–384.

Morilla, M.J., Benavidez, P., Lopez, M., Bakas, L., Romero, E., 2002. Development and in vitro characterisation of a benznidazole liposomal formulation. Int. J. Pharm. 249, 89–99.

Morilla, M.J., Montanari, J., Prieto, M., Lopez, M., Petray, P., Romero, E., 2004. Intravenous liposomal benznidazole as trypanocidal agent: increasing drug delivery to liver is not enough. Int. J. Pharm. 278, 311–318.

Moustafine, R., 2011. Interpolymer combinations of chemically complementary grades of Eudragit copolymers: a new direction in the design of peroral solid dosage forms of drug delivery systems with controlled release (review). Pharm. Chem. J. 45, 285–295.

Moustafine, R., Bukhovets, A., Sitenkov, A.Y., Garipova, V., Kemenova, V., Rombaut, P., Van den Mooter, G., 2011. Synthesis and characterization of a new carrier based on Eudragit® EPO/S100 interpolyelectrolyte complex for controlled colon-specific drug delivery. Pharm. Chem. J. 45, 568–574.

Moustafine, R.I., Kemenova, V., Van den Mooter, G., 2005. Characteristics of interpolyelectrolyte complexes of Eudragit E 100 with sodium alginate. Int. J. Pharm. 294, 113–120.

Moustafine, R.I., Margulis, E.B., Sibgatullina, L.F., Kemenova, V.A., Van den Mooter, G., 2008. Comparative evaluation of interpolyelectrolyte complexes of chitosan with Eudragit® L100 and Eudragit® L100–55 as potential carriers for oral controlled drug delivery. Eur. J. Pharm. Biopharm. 70, 215–225.

Nista, S.V.G., Bettini, J., Mei, L.H.I., 2015. Coaxial nanofibers of chitosan–alginate–PEO polycomplex obtained by electrospinning. Carbohydrate polymers 127, 222–228.

Nogami, H., Nagai, T., Fukuoka, E., Sonobe, T., 1969. Disintegration of the aspirin tablets containing potato starch and microcrystalline cellulose in various concentrations. Chem. Pharm. Bull. 17, 1450–1455.

Obeidat, W.M., Abu Znait, A.a.H., Sallam, A.-S.A., 2008. Novel combination of anionic and cationic polymethacrylate polymers for sustained release tablet preparation. Drug Dev. Ind. Pharmacy 34, 650–660..

Olivera, M.E., Manzo, R.H., Alovero, F., Jimenez-Kairuz, A.F., Ramírez-Rigo, M.V., 2017. Polyelectrolyte-drug ionic complexes as nanostructured drug carriers to design solid and liquid oral delivery systems. In: Andronescu, E., Grumezescu, A.M. (Eds.), Nanostructures for Oral Medicine, first ed. Elsevier, pp. 365–408.

Pagels, R.F., Prud'homme, R.K., 2015. Polymeric nanoparticles and microparticles for the delivery of peptides, biologics, and soluble therapeutics. J. Control. Release 219, 519–535.

Palena, M., García, M., Manzo, R., Jimenez-Kairuz, A., 2015. Self-organized drug-interpolyelectrolyte nanocomplexes loaded with anionic drugs. Characterization and in vitro release evaluation. J. Drug Delivery Sci. Technol. 30 (Part A), 45–53.

Palmeiro-Roldán, R., Fonseca-Berzal, C., Gómez-Barrio, A., Arán, V.J., Escario, J.A., Torrado-Durán, S., Torrado-Santiago, S., 2014. Development of novel benznidazole formulations: physicochemical characterization and in vivo evaluation on parasitemia reduction in Chagas disease. Int. J. Pharm. 472, 110–117.

Pan, X., Chen, M., Han, K., Peng, X., Wen, X., Chen, B., Wang, J., Li, G., Wu, C., 2010. Novel compaction techniques with pellet-containing granules. Eur. J. Pharm. Biopharm. 75, 436–442.

Peppas, N., 1985. Analysis of Fickian and non-Fickian drug release from polymers. Pharm. Acta Helv. 60, 110.

Pérez, P., Suñé-Negre, J.M., Miñarro, M., Roig, M., Fuster, R., García-Montoya, E., Hernández, C., Ruhí, R., Ticó, J.R., 2006. A new expert systems (SeDeM Diagram) for control batch powder formulation and preformulation drug products. Eur. J. Pharm. Biopharm. 64, 351–359.

Prado, H., Matulewicz, M., Bonelli, P., Cukierman, A., 2008. Basic butylated methacrylate copolymer/kappa-carrageenan interpolyelectrolyte complex: preparation, characterization and drug release behaviour. Eur. J. Pharm. Biopharm. 70, 171–178.

Raafat, D., Sahl, H.G., 2009. Chitosan and its antimicrobial potential–a critical literature survey. Microb. Biotechnol. 2, 186–201.

Ramirez-Rigo, M., Allemandi, D., Manzo, R., 2006. Swellable drug-polyelectrolyte matrices (SDPM) of alginic acid characterization and delivery properties. Int. J. Pharm.

Rassi, A.J., Rassi, A., de Rezende, J.M., 2012. American trypanosomiasis (Chagas disease). Infect. Dis. Clinics North America 26, 275–291.

Rassi, A.J., Rassi, A., Marin-Neto, J., 2010. Chagas disease. Lancet 375, 1388–1402.

Retsch GmbH, 2017. International Comparison Table for Test Sieves. Test Sieve Comparison Table for Standards.

Rojo, G., Castillo, C., Duaso, J., Liempi, A., Droguett, D., Galanti, N., Maya, J., Lopez-Munoz, R., Kemmerling, U., 2014. Toxic and therapeutic effects of Nifurtimox and Benznidazol on *Trypanosoma cruzi* ex vivo infection of human placental chorionic villi

explants. Acta Trop. 132, 112–118.
Sá-Barreto, L.C., Gustmann, P.C., Garcia, F.S., Maximiano, F.P., Novack, K.M., Cunha-Filho, M.S., 2013. Modulated dissolution rate from the inclusion complex of anticchagasic benznidazole and cyclodextrin using hydrophilic polymer. Pharm. Dev. Technol. 18, 1035–1041.
Sakurai, K., Maegawa, T., Takahashi, T., 2000. Glass transition temperature of chitosan and miscibility of chitosan/poly (N-vinyl pyrrolidone) blends. Polymer 41, 7051–7056.
Severino, P., de Oliveira, G.G., Ferraz, H.G., Souto, E.B., Santana, M.H., 2012. Preparation of gastro-resistant pellets containing chitosan microspheres for improvement of oral didanosine bioavailability. J. Pharm. Anal. 2, 188–192.
Siepmann, J., Peppas, N., 2001. Modeling of drug release from delivery systems based on hydroxypropyl methylcellulose (HPMC). Adv. Drug Delivery Rev. 48, 139–157.
Soares-Sobrinho, J.L., Santos, F.L., Lyra, M.A., Alves, L.D., Rolim, L.A., Lima, A.A., Nunes, L.C., Soares, M.F., Rolim-Neto, P.J., Torres-Labandeira, J.J., 2012. Benznidazole drug delivery by binary and multicomponent inclusion complexes using cyclodextrins and polymers. Carbohydr. Polym. 89, 323–330.
Staniforth, J., 2002. Powder flow. In: Aulton, M.E. (Ed.), Pharmaceutics: The Science of Dosage Form Design, 2° ed. Churchill Livingstone Elsevier Science Limited, España, pp. 197–210.
Streck, L., de Araújo, M.M., de Souza, I., Fernandes-Pedrosa, M.F., do Egito, E.S.T., de Oliveira, A.G., da Silva-Júnior, A.A., 2014. Surfactant–cosurfactant interactions and process parameters involved in the formulation of stable and small droplet-sized benznidazole-loaded soybean O/W emulsions. J. Mol. Liq. 196, 178–186.
Takeuchi, H., Thongborisute, J., Matsui, Y., Sugihara, H., Yamamoto, H., Kawashima, Y., 2005. Novel mucoadhesion tests for polymers and polymer-coated particles to design optimal mucoadhesive drug delivery systems. Adv. Drug Delivery Rev. 57, 1583–1594.
Thakur, V.K., Thakur, M.K., 2014. Recent advances in graft copolymerization and applications of chitosan: a review. ACS Sustain. Chem. Eng. 2, 2637–2652.
U.S. Pharmacopoeial Convention, 2015. United States Pharmacopoeia (38). The National Formulary and Dispensing Information (33) United States Pharmacopeia Convention Inc., Rockville, Maryland.
Vila Jato, J., 1997. Tecnología Farmacéutica-Aspectos fundamentales de los sistemas farmacéuticos y operaciones básicas. Editorial Síntesis, Madrid, pp. 75–142.
Wang, Z., Zhang, X., Gu, J., Yang, H., Nie, J., Ma, G., 2014. Electrodeposition of alginate/chitosan layer-by-layer composite coatings on titanium substrates. Carbohydr. Polymers 103, 38–45.
World Health Organization, W., 2015. The international pharmacopoeia, 5° ed. World Health Organization.
Zargar, V., Asghari, M., Dashti, A., 2015. A review on chitin and chitosan polymers: structure, chemistry, solubility, derivatives, and applications. ChemBioEng Rev. 2, 204–226.